ELSEVIER

Journal of Quantitative Spectroscopy & Radiative Transfer 89 (2004) 421–442

Journal of Quantitative Spectroscopy & Radiative Transfer

www.elsevier.com/locate/jqsrt

A new look at anomalous diffraction theory (ADT): Algorithm in cumulative projected-area distribution domain and modified ADT

Ping Yang[a,*], Zhibo Zhang[a], Bryan A. Baum[b], Hung-Lung Huang[c], Yongxiang Hu[b]

[a]*Department of Atmospheric Sciences, Texas A&M University, TAMU 3150, College Station, TX 77843, USA*
[b]*NASA Langley Research Center, Hampton, VA 23681, USA*
[c]*Cooperative Institute for Meteorological Satellite Studies, University of Wisconsin-Madison, 1225 W. Dayton Street, Madison, WI 53706, USA*

Abstract

Two recent papers (Opt. Lett. 28 (2003) 179; Appl. Opt. 42 (2003) 6710) show that the conventional anomalous diffraction theory (ADT) can be reformulated by using the probability distribution function of the geometrical paths of rays inside a scattering particle. In this study we further enhance the new ADT formulation by introducing a dimensionless scaled projectile-length ($\tilde{l}_q$) defined in the domain of the cumulative projected-area distribution (q) of a particle. The quantity $\tilde{l}_q$ contains essentially all the information about particle shape and aspect ratio, which, however, is independent of particle dimension (e.g., large and small spheres have the same $\tilde{l}_q$). With this feature of $\tilde{l}_q$, the present ADT algorithm is computationally efficient if a number of particle sizes and wavelengths are considered, particularly when a random orientation condition is assumed. Furthermore, according to the fundamental ADT assumption regarding the internal field within a scattering particle, we modify ADT on the basis of two rigorous relationships that relate the extinction and absorption cross sections to the internal field. Two tuning factors are introduced in the modified ADT solution, which can be determined for spheres by fitting the modified ADT results to the corresponding Lorenz-Mie solutions. For nonspherical particles, the tuning factors obtained for spheres can be used as surrogates. This approach is tested for the case of circular

*Corresponding author. Tel.: +1-979-845-4923; fax: +1-979-862-4466.
E-mail address: pyang@ariel.met.tamu.edu (P. Yang).

0022-4073/$ - see front matter © 2004 Elsevier Ltd. All rights reserved.
doi:10.1016/j.jqsrt.2004.05.038

cylinders whose optical properties can be accurately calculated from the T-matrix method. Numerical computations show that the modified ADT solution is more accurate than its conventional ADT counterpart.
© 2004 Elsevier Ltd. All rights reserved.

Keywords: Anomalous diffraction theory; Algorithm; Extinction and absorption

1. Introduction

Although a number of rigorous methods (see, Wriedt [1], Mishchenko et al. [2], Kahnert [3], and references cited therein) have been developed for calculating the optical properties of nonspherical particles, the anomalous diffraction theory (ADT) originally developed by van de Hulst [4] is still an effective alternative for the computation of the extinction and absorption cross sections of a particle when it is optically tenuous. The popularity of ADT is demonstrated by the number of recent publications on this subject [5–15, e.g.]. The merits of ADT are its simplicity in concept and efficiency in numerical computation, although this method suffers some shortcomings, such as missing the above-edge contribution as illustrated by Baran et al. [16]. Mitchell [17] has substantially improved the accuracy of ADT in the spherical case by parameterizing the missing physics, specifically, the internal reflection/refraction, photon tunneling, and edge diffraction. The edge effect has been previously investigated by Jones [18,19] and Nussenzveig and Wiscombe [20]. Most recently, Zhao and Hu [21] developed a general bridging technique to include the particle edge contribution in the ADT computation.

In the ADT framework, the incident electromagnetic wave can be regarded as a number of small localized waves that propagate towards a scattering particle along the incident direction without divergence. The path of a localized wave, a straight ray-tube with a finite cross section, is referred to as a projectile. The propagating direction and polarization configuration of the internal field inside the particle are assumed to be the same as those of the incident wave. However, the internal field suffers a phase delay due to the presence of the scattering particle. The extinction cross section is associated with the phase interference of the individual projectiles, whereas the corresponding absorption cross section is the summation of the absorption of all the projectiles. For well-defined regular geometries such as spheres [4], spheroids [8], circular cylinders [9–11], cubes [12,13] and hexagons [14], analytical ADT solutions can be obtained. It is unlikely that an analytical ADT solution can be derived for a general nonspherical geometry. Thus, a numerical method must be used to account for the contributions of individual projectiles. The accuracy of the numerical computation depends on the dimensions of the cross sections of the projectiles. In practice, the linear dimensions of the projectiles need to be much smaller than the incident wavelength so that one can account accurately for the coherent phase interference of the transmitted wave that penetrates the particle. If the size parameter (i.e., the ratio of particle size to the incident wavelength) is large, however, the number of the projectiles required can be extremely high, leading to a significant computational effort. The computational burden may be further aggravated if the numerical computation needs to be reiterated for various size parameters and spectral wavelengths, particularly when a random orientation condition is assumed for the particles.

The computation of the extinction and absorption cross sections in the ADT framework is independent of the order in which the contributions of individual projectiles are accounted for. For example, the ADT solution to the absorption cross section, given by a discrete summation of the absorption of individual projectiles used in the numerical computations, is irrelevant to the order of the projectiles in the summation. Furthermore, the projected-area distribution (i.e., the percentage of the particle projected area that corresponds to the projectile-length in a specific interval) is independent of the particle's physical size if the shape and aspect ratio of the particle remain the same. These features allow ADT to be formulated in a more computationally efficient manner. Most recently, Xu et al. [22] and Xu [23] introduced the probability distribution function of the geometric paths of rays inside particles and reformulated the conventional ADT solutions for the extinction and absorption cross sections of a particle. In terms of methodology, we notice that the conventional ADT formulation and that developed by Xu et al. [22] are similar to the line-by-line method and the k-distribution method, respectively. The line-by-line and k-distribution methods are developed for calculating the gaseous spectral transmittance over a given wavenumber interval. The details of the line-by-line and k-distribution methods can be found in Goody and Yung [24], Liou [25], Chou and Kouvaris [26], Lacis and Oinas [27], Fu and Liou [28], and Kratz [29]. Furthermore, we notice that the new ADT formulation developed by Xu et al.[22] can be further enhanced to increase the computational efficiency.

There are two goals for this study. First, to enhance the algorithm developed by Xu et al.[22] and Xu [23], we introduce a dimensionless scaled projectile-length ($\tilde{l}_q$) that is specified in the domain of cumulative projected-area distribution (q). The scaled projectile length quantitatively describes the behaviors of the distribution of projectile-length inside the particle. Using $\tilde{l}_q$, we develop a computationally efficient ADT algorithm. Second, to reduce the errors of ADT for its implementation for moderate refractive indices, we also modify the conventional ADT formulation by applying the ADT assumption for the internal field to two rigorous relationships in classic electrodynamics, which relate the extinction and absorption cross sections to the internal electric field inside the particle.

This paper proceeds as follows. Section 2 presents the general ADT formulation in the domain of the projectile-length distribution. A modified ADT method is presented in Section 3, and Section 4 summarizes this study.

2. ADT algorithm in cumulative projected-area distribution domain

2.1. General formulation

The physical rationale associated with ADT for computing the extinction and absorption cross sections (or efficiencies) of optically tenuous large particles has been well explained by van de Hulst [4]. Without recapturing the physical base and the applicability criteria for ADT, we present the conventional ADT formulae for computing the extinction and absorption cross sections of an

arbitrarily shaped particle with a specific orientation as follows:

$$C_{\text{ext}} = 2\text{Re}\left\{\int\int_P [1 - e^{ikl(m-1)}]\,dP\right\},$$
$$= 2\int\int_P \{1 - e^{-klm_i}\cos[kl(m_r - 1)]\}\,dP \tag{1}$$

and

$$C_{\text{abs}} = \int\int_P (1 - e^{-2klm_i})\,dp, \tag{2}$$

where $k = 2\pi/\lambda$ is the wave constant in which λ is the incident wavelength, $m = m_r + im_i$ is the complex refractive index of the particle, m, is the imaginary part of m. The integral domain in Eqs. (1) and (2) are the projected area of the particle on a plane perpendicular to the incident direction, and l is the length of the projectile segment within the particle.

As shown in Fig. 1, the incident wave is along the z-axis. The projectile-length within the scattering particle can be expressed as follows:

$$l = \hat{z}\cdot(\vec{r} - \vec{r}_0) = l(x, y), \tag{3}$$

where $\hat{z}$ is a unit vector along the z axis. The projectile-length, $l(x, y)$, depends on the location where the incident projectile intercepts with a plane normal to the incident direction (i.e., the plane P in Fig. 1). Analytical solutions to Eqs. (1) and (2) can be obtained for a limited set of particle shapes such as spheres, spheroids, circulars, cylinders, cubes and hexagons. For more complicated geometries that are quite often found in nature, such as bullet rosette ice crystals in cirrus clouds [30,31], it is likely that a numerical method has to be used to evaluate the integrals in Eqs. (1) and (2). Since the value of the extinction cross section is sensitive to the phase interference of the transmitted wave, a fine resolution grid must be used to resolve the variation of the projectile-length from its initial point (x, y) within the projected area of the particle on a plane normal to the incident direction. Thus, the projected area of the particle needs to be divided into an enormous number of projectiles for the case of a moderate or large size parameter. The integrals in Eqs. (1) and (2) are computed by discrete summations of the contributions from individual projectiles. This approach is not efficient computationally if multiple particle sizes and wavelengths are involved, particularly when random orientations are assumed for particles with sizes much larger than the incident wavelength. To overcome this issue, we start with the ADT formulation developed by Xu et al. [22] and Xu [23], which is given as follows:

$$C_{\text{ext}} = 2\text{Re}\{P\int[1 - e^{ikl(m-1)}f(l)]\,dl\}, \tag{4}$$

and

$$C_{\text{abs}} = P\int(1 - e^{-2klm_i})f(l)\,dl, \tag{5}$$

where P is the projected area of the particle. The quantity $f(l)$ is interpreted by Xu et al. [22] and Xu [23] as the probability distribution function of the geometrical paths of rays inside the particle,

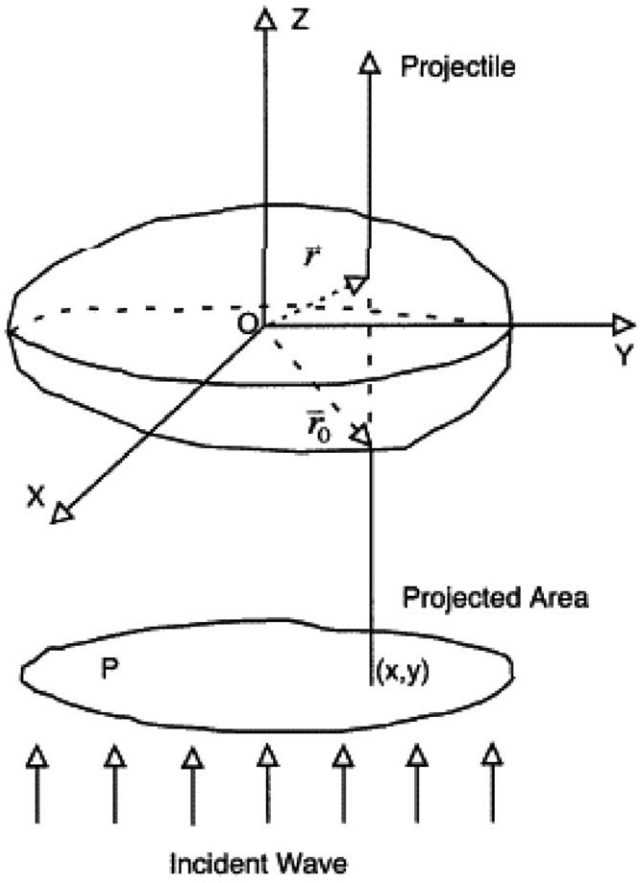

Fig. 1. Geometric configuration illustrating the principle of the anomalous diffraction theory.

since the anomalous diffraction extinction of light is viewed as a statistical process. The quantity $f(l)$ can also be thought of as the fraction of particle projected area when the projectile-length is between $l - \mathrm{d}l/2$ and $l + \mathrm{d}l/2$, since the extinction and absorption processes associated with Eqs. (1) and (2) are deterministic processes. It is interesting to note that the transform from Eqs. (1) and (2) to Eqs. (4) and (5) is similar to the transform from the line-by-line method to the k-distribution method developed for the computation of the mean gaseous transmittance for a given spectral interval. The mean transmittance can be computed by integrating the monochromatic transmittance in the wavenumber domain, an approach known as the line-by-line method. Alternatively, it can be computed in the k (absorption coefficient) or cumulative k distribution (g) domain (i.e., the so-called k-distribution method). The absorption coefficient k is usually a rapidly oscillating function in the wavenumber domain whereas the absorption coefficient is a smooth function in the g domain. Thus, it requires much fewer quadrature points to calculate the spectral transmittance in the g domain than in the wavenumber domain. To adopt the methodology of the k-distribution method to improve the efficiency of ADT, Eqs. (4) and (5)

are rewritten as follows:

$$C_{\text{ext}} = 2\text{Re}\left\{ P \int_0^1 \{1 - \mathrm{e}^{\mathrm{i}kl_{\max}\tilde{l}(m-1)} f(\tilde{l})\}\, \mathrm{d}\tilde{l} \right\}$$
$$= 2P \int_0^1 \{1 - \mathrm{e}^{-kl_{\max}\tilde{l}m_i} \cos[kl_{\max}\tilde{l}(m_r - 1)]\} f(\tilde{l})\, \mathrm{d}\tilde{l}, \tag{6}$$

and

$$C_{\text{abs}} = P \int_0^1 (1 - \mathrm{e}^{-2kl_{\max}\tilde{l}m_i}) f(\tilde{l})\, \mathrm{d}\tilde{l}, \tag{7}$$

where $l_{\max}$ is the maximum projectile-length for a particle with a given orientation; $\tilde{l}$, the scaled projectile-length, is a dimensionless quantity, given by $\tilde{l} = l/l_{\max}$. For simplicity in the present formulation without losing generality, we assume that the minimum projectile-length ($l_{\min}$) is zero. In the case when the minimum projectile-length is nonzero, the lower integral-limit in Eqs. (6) and (7) should be $\tilde{l}_{\min} = l_{\min}/l_{\max}$. The quantity $f(\tilde{l})$ in Eqs. (6) and (7) is the fraction (percentage) of the projected area (P) when the projectile-length is between $l_{\max}(\tilde{l} - \mathrm{d}\tilde{l}/2)$ and $l_{\max}(\tilde{l} + \mathrm{d}\tilde{l}/2)$. Note that $f(\tilde{l})$ is normalized, that is, the following normalization condition holds:

$$\int_0^1 f(\tilde{l})\, \mathrm{d}\tilde{l} = 1. \tag{8}$$

Furthermore, we define the cumulative fraction q associated with $f(\tilde{l})$ as follows:

$$q(\tilde{l}) = \int_0^{\tilde{l}} f(\tilde{l}')\, \mathrm{d}\tilde{l}', \tag{9a}$$

or,

$$\mathrm{d}q = f(\tilde{l})\, \mathrm{d}\tilde{l}. \tag{9b}$$

Because $f(\tilde{l})$ is a non-negative quantity, q defined by Eq. (9a) is a monotonically increasing function of $\tilde{l}$. Thus, there is a one-to-one mapping between $\tilde{l}$ and q for the range $\tilde{l} \in [0, 1]$. By taking the inverse of the cumulative distribution function, we can express $\tilde{l}$ as a function of q, that is

$$\tilde{l}_q = \tilde{l}(q), \tag{10}$$

where the subscript q indicates that the scaled projectile length is expressed in the q domain. From Eqs. (6), (9b) and (11), the extinction cross section in the ADT frame can thus be given as follows:

$$C_{\text{ext}} = 2P\text{Re}\left\{ \int_0^1 [1 - \mathrm{e}^{ikl_{\max}\tilde{l}_q(m-1)}]\, \mathrm{d}q \right\}$$
$$= 2P \int_0^1 \{1 - \mathrm{e}^{-kl_{\max}\tilde{l}_q m_i} \cos[kl_{\max}\tilde{l}_q(m_r - 1)]\}\, \mathrm{d}q. \tag{11}$$

Similarly, for the absorption cross section, we have

$$C_{\mathrm{abs}} = P \int_0^1 \mathrm{e}^{-2kl_{\max}\tilde{l}_q m_i}\,\mathrm{d}q. \tag{12}$$

The extinction and absorption efficiencies corresponding to Eqs. (11) and (13) are given by

$$Q_{\mathrm{ext}} = C_{\mathrm{ext}}/P = 2\int_0^1 [1 - e^{-kl_{\max}\tilde{l}_q m_i}\cos kl_{\max}\tilde{l}_q(m_r - 1)]\,\mathrm{d}q, \tag{13}$$

and

$$Q = C_{\mathrm{abs}}/P = \int_0^1 \mathrm{e}^{-2kl_{\max}\tilde{l}_q m_i}\,\mathrm{d}q. \tag{14}$$

Note that Eqs. (11)–(15) are general expressions without being limited to a specific geometry. Furthermore, the scaled projectile-length in the q domain is independent of the particle physical size (e.g., $\tilde{l}_q$ is the same for a sphere with a radius of 100 μm as for one with a radius of 5 μm). This feature implies that the computational effort can be reduced substantially if a range of particle sizes is involved. For a given geometry, the key computational effort in the present method is to derive the scaled projectile-length in the domain, which is defined by Eq. (11). As the simplest example, Fig. 2 illustrates how to obtain $\tilde{l}_q$ in the case for a sphere. The maximum projectile-length for a sphere is

$$l_{\max} = 2R, \tag{15}$$

where R is the radius of the sphere. From the geometric configuration shown in Fig. 2, we have

$$l = 2R\cos\eta = l_{\max}\cos\eta. \tag{16}$$

The corresponding scaled projectile-length is given by

$$\tilde{l} = l/l_{\max} = \cos\eta. \tag{17}$$

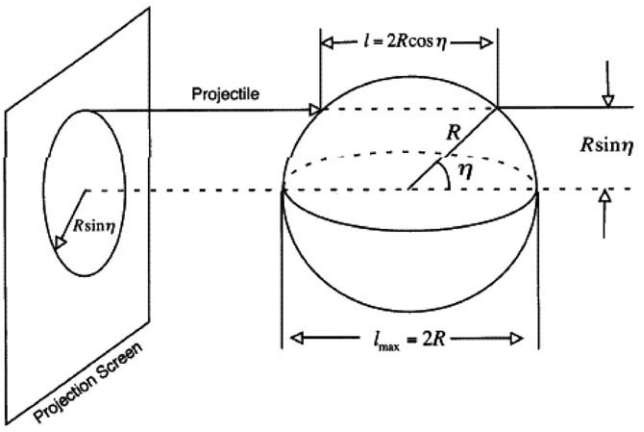

Fig. 2. Geometry for deriving the distribution function of particle projected area as a function of the projectile-length.

The fraction of the projected area, when the projectile-length is between $l_{\max}$ and l, is given by

$$A = \pi R^2 \sin^2\eta = \pi R^2(1-\tilde{l}^2). \tag{18}$$

According to the physical meaning of $f(\tilde{l})$, we have

$$f(\tilde{l}) = \left|\frac{1}{\pi R^2}\frac{\mathrm{d}A}{\mathrm{d}\tilde{l}}\right| = 2\tilde{l}. \tag{19}$$

The corresponding cumulative fraction of the projected area, q, is given by

$$q(\tilde{l}) = \int_0^{\tilde{l}} f(\tilde{l}')\,\mathrm{d}\tilde{l}' = \tilde{l}^2. \tag{20}$$

From Eqs. (18) and (21), q is in the range of [0,1] because of $\tilde{l} \in [0,1]$. The projectile-length in the q domain is given by

$$\tilde{l}_q = q^{1/2}. \tag{21}$$

It can be seen that the scaled projectile-length $\tilde{l}_q$ is independent of the physical size of a sphere. The ADT solutions to the extinction and absorption cross sections of a sphere in the q domain are given as follows:

$$C_{\mathrm{ext}} = 2P\mathrm{Re}\left\{\int_0^1 \{1-\exp[\mathrm{i}kl_{\max}q^{1/2}(m-1)]\}\,\mathrm{d}q\right\}, \tag{22}$$

and

$$C_{\mathrm{abs}} = P\int_0^1 [1-\exp(-2kl_{\max}q^{1/2}m_i)]\,\mathrm{d}q. \tag{23}$$

To show the equivalence of the preceding expressions to those given by the conventional ADT, let $q = \sin^2\xi$ and $w = -\mathrm{i}kl_{\max}(m-1)$. The integral in Eq. (23) then reduces to the following form

$$\begin{aligned} C_{\mathrm{ext}} &= 4P\mathrm{Re}\left\{\int_0^{\frac{\pi}{2}}(1-\mathrm{e}^{-w\sin\xi})\cos\xi\sin\xi\,\mathrm{d}\xi\right\} \\ &= 4P\mathrm{Re}\left(\frac{1}{2}+\frac{\mathrm{e}^{-w}}{w}+\frac{\mathrm{e}^{-w}-1}{w^2}\right). \end{aligned} \tag{24}$$

The result given by Eq. (24) is exactly the same as the form given by van de Hulst [4]. Similarly, the absorption cross section can be expressed as follows:

$$\begin{aligned} C_{\mathrm{abs}} &= 2P\int_0^{\frac{\pi}{2}}(1-\mathrm{e}^{-u\sin\xi})\cos\,\xi\,\sin\,\xi\,\mathrm{d}\xi \\ &= 2P\left(\frac{1}{2}+\frac{\mathrm{e}^{-u}}{u}+\frac{\mathrm{e}^{-u}-1}{u^2}\right), \end{aligned} \tag{25}$$

where $u = 2kl_{\max}m_i$. Again, in the computation of the absorption cross section, the present formulation is equivalent to its conventional ADT counterpart [4].

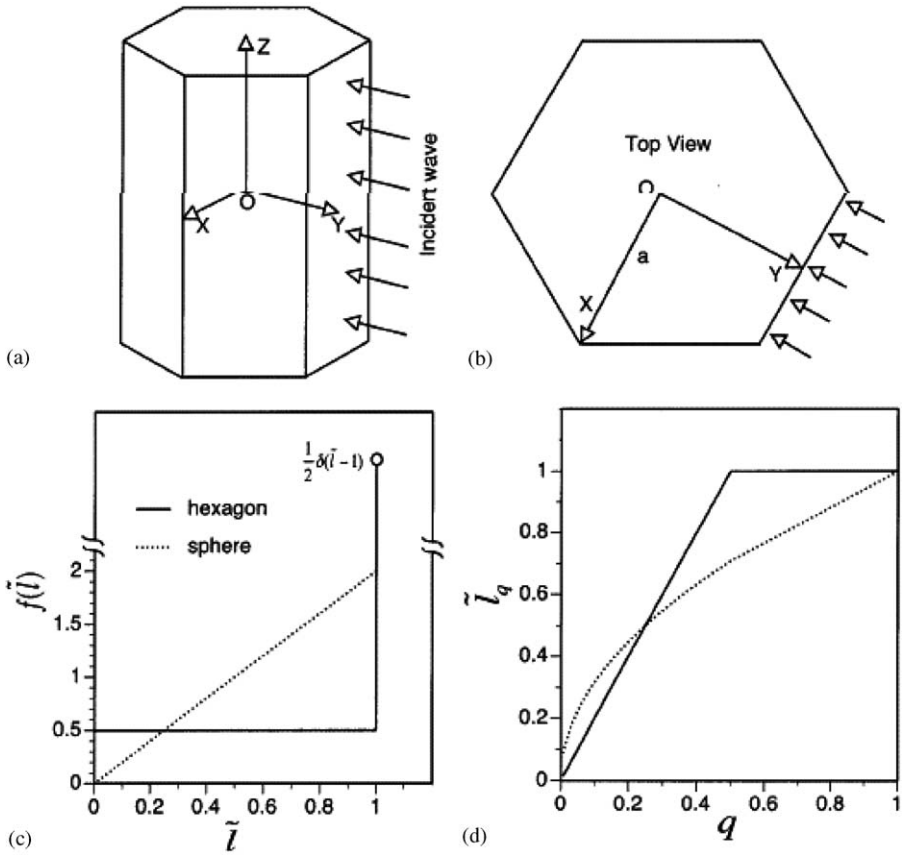

Fig. 3. (a) and (b): the incident configuration for the ADT computation in a case for a specifically oriented hexagon; (c): projected-area distribution function, $f(\tilde{l})$, for a sphere and a hexagon whose orientation is specified in (a) and (b); (d): scaled projectile-length associated with $f(\tilde{l})$ in (c).

Fig. 3 illustrates the computation of $f(\tilde{l})$ and $\tilde{l}_q$ in a case for a hexagonal geometry that is quite interesting to atmospheric research because pristine ice crystals often possess hexagonal structures. Figs. 3(a) and (b) show the orientation of the particle relative to the incident projectiles. The incident direction is perpendicular to the symmetry-axis of the particle and faces the broad side of the particle's cross section. Thus, the ADT configuration associated with Figs. 3(a) and (b) actually reduces to a 2-D case. It is evident from Fig. 3(b) that the maximum projectile-length is $l_{\max} = \sqrt{3}a$ in which a is the semi-width of the particle's cross section. The ratio of the area associated with $l_{\max}$ (i.e., the case when a projectile passes through two faces that are parallel to each other) to the total projected area is 50%. The other half of the projected area corresponds to $\tilde{l} \in [0, 1)$, a region that excludes the point $\tilde{l} = 1$. Thus, the exact solution for $f(\tilde{l})$ is given as follows:

$$f(\tilde{l}) = \frac{1}{2} + \frac{1}{2}\delta(\tilde{l} - 1), \tag{26}$$

where δ is the Dirac delta function. From Eqs. (9a), (11) and (27), the scaled projectile-length in the q domain can be given in the form of

$$\tilde{l}_q = \begin{cases} 2q, & \text{for } 0 \leqslant q \leqslant 0.5, \\ 1, & \text{for } q > 0.5. \end{cases} \tag{27}$$

Fig. 3(c) and 3(d) show $f(\tilde{l})$ and $\tilde{l}_q$ given by Eqs. (27) and (28), respectively, which are compared with their spherical counterparts. The effect of particle geometry on the distribution of projectile-length is pronounced. As explained in the previous discussion, $f(\tilde{l})$ and $\tilde{l}_q$ are independent of particle physical size. Thus, it is not proper to approximate a nonspherical particle with a specific orientation using a sphere regardless of the definition of ''spherical equivalence'' (i.e., how a spherical radius is specified for the ''equivalence'') in the computation of the extinction and absorption cross sections in the ADT frame.

Results from the present ADT algorithm for the case for a nonspherical particle, specifically for a hexagonal ice crystal with the incident configuration shown in Fig. 3, can be compared to the analytical ADT solution derived by Sun and Fu [14]. The results are shown in Fig. 4 for the extinction and absorption cross sections computed at a wavelength of 3.7 μm. The refractive index of ice [32] at this wavelength is $m = 1.4 + 0.0072\mathrm{i}$. The two results are exactly the same, as is evident from Fig. 4 in which the solid and dotted lines are overlapped. For an arbitrary nonspherical geometry, it is difficult to obtain an analytical expression for $f(\tilde{l})$ or $\tilde{l}_q$. In this case, a numerical approach has to be used. Specifically, a rectangular area that bounds the projectile projection on a plane normal to the incident direction is divided into a number of small area elements (uniform square area elements in practice). Then it is determined whether the projectiles associated with the small area elements interact with the particle. A projectile is disregarded in the numerical computation if it does not strike the scattering particle; that is, only those projectiles impinging on the particle are accounted for. We divide the range [0, 1] into n uniform intervals for $\tilde{l}$; that is, the width of the interval is given by $\Delta\tilde{l} = 1/n$. The projectile-lengths of all the projectiles

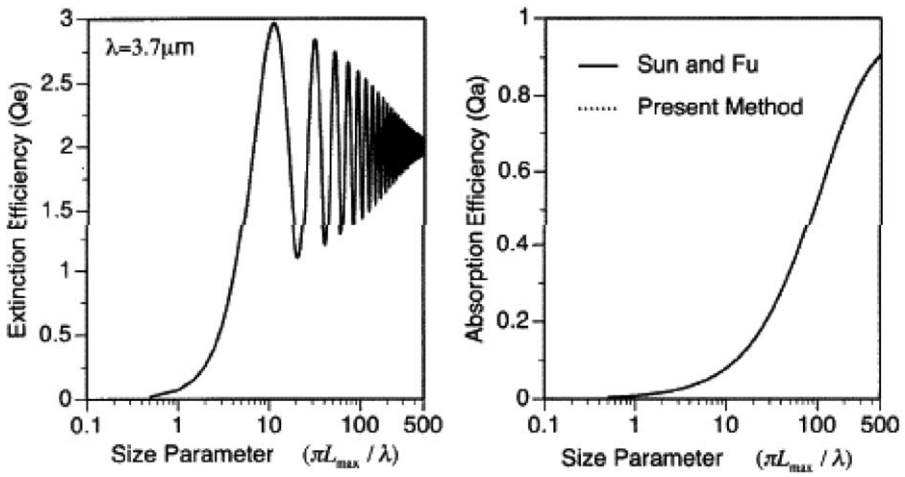

Fig. 4. Comparison of extinction and absorption efficiencies (Q_{ext} and Q_{abs}) computed from the present ADT method in the q domain and from an analytical ADT solution reported by Sun and Fu [14].

that impinge on the particle are calculated sequentially. Let the number of the projectiles whose lengths within the particle are between $(j-1)\Delta\tilde{l}$ and $j\Delta\tilde{l}$ be N_j. Thus, we have

$$f[(j-1/2)\Delta\tilde{l}] = \frac{N_j}{\Delta\tilde{l}\sum_{i=1}^{n} N_i}. \tag{28}$$

The corresponding cumulative projected area distribution function q is given by

$$q_j = q[j\Delta\tilde{l}] = \sum_{k=1}^{j} \Delta\tilde{l} f[(k-1/2)\Delta\tilde{l}] = \frac{\sum_{k=1}^{j} N_k}{\sum_{i=1}^{n} N_i}. \tag{29}$$

From Eq. (30), the numerical pairs of $(\tilde{l}_j, q_j)$ with $\tilde{l}_j = j\Delta\tilde{l}$ are obtained; i.e., the dimensionless scaled projectile-length in the q domain is obtained, as $\tilde{l}_j$ can be regarded as a discrete value of the function $\tilde{l}(q)$ at $q = q_j$.

2.2. Randomly oriented particles

Consider an ensemble of nonspherical particles that are randomly oriented in space. As shown in Fig. 5, the orientation of a nonspherical particle relative to the laboratory coordinate system, $oxyz$, can be specified in terms of three angles: θ_p, φ_p, and β. The extinction and absorption cross sections in the ADT frame for a specific orientation of the particle depend on angles θ_p and β (note that in a rigorous scattering theory the extinction and absorption cross sections also depend

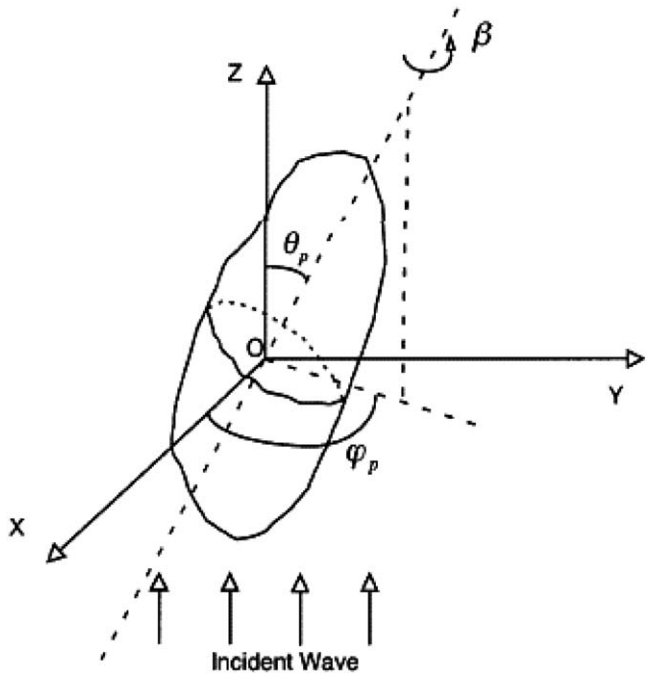

Fig. 5. Conceptual diagram showing the orientation of a nonspherical particle with respect to the incident direction.

on the polarization configuration of the incident wave, i.e., the φ_p-dependence is involved). In the conventional ADT algorithm, the ensemble-averaged (or orientation-averaged) extinction cross section is given as follows:

$$\langle C_{\text{ext}}\rangle = 2(4\pi)^{-1}\text{Re}\left\{\int_0^{2\pi}\int_0^{\pi}\int\int_P [1-\text{e}^{\text{i}kl(m-1)}]\,\text{d}x_p\,\text{d}y_p\sin\theta_p\,\text{d}\theta_p\,\text{d}\beta\right\}, \tag{30}$$

where the integration over $\text{d}x_p\text{d}y_p$ is carried out over the particle projected area. The preceding expression is inefficient computationally since a four-order integral is involved. Moreover, integration has to be repeated if various particle sizes are considered for multiple spectral wavelengths. With the approach based on the distribution of projectile-length, the extinction cross section given by Eq. (31) can be rewritten as follows:

$$\langle C_{\text{ext}}\rangle = 2(4\pi)^{-1}\text{Re}\left\{\int_0^{2\pi}\int_0^{\pi} P(\theta_P,\beta)\int_0^1 [1-\text{e}^{\text{i}kl_{\max}(\theta_p,\beta)\tilde{l}(m-1)}]f(\tilde{l})\,\text{d}\tilde{l}\sin\theta_p\,\text{d}\theta_p\,\text{d}\beta\right\}, \tag{31}$$

where $l_{\max}(\theta_p,\beta)$ is the maximum projectile-length for a specific particle orientation associated with angles θ_p and β (see Fig. 5).

In the case for randomly orientated particles, we define the maximum projectile-length for an ensemble of the particles as follows:

$$L_{\max} = \max[l_{\max}(\theta_p,\beta)] \quad \text{for } \theta_p\in[0,\pi] \text{ and } \beta\in[0,2\pi]. \tag{32}$$

The dimensionless scaled projectile-length for the ensemble is

$$\tilde{L} = l_{\max}(\theta_p,\beta)\tilde{l}/L_{\max}. \tag{33}$$

The projectile-length distribution, $f(\tilde{l})$, averaged over particle orientations, is given by

$$\overline{f}(\tilde{L}) = (4\pi\overline{P})^{-1}\int_0^{2\pi}\int_0^{\pi} P(\theta_p,\beta)f(\tilde{L})\sigma[l_{\max}(\theta_p,\beta)/L_{\max}-\tilde{L}]\sin\theta_p\,\text{d}\theta_p\,\text{d}\beta, \tag{34}$$

where $\overline{P}$ is the ensemble-averaged projected area, given by

$$\overline{P} = (4\pi)^{-1}\int_0^{2\pi}\int_0^{\pi} P(\theta_p,\beta)\sin\theta_p\,\text{d}\theta_p\,\text{d}\beta. \tag{35}$$

For a convex geometry, $\overline{P}$ is $S/4$, in which S is the surface area of the geometry [33]. The function in Eq. (35) is a step function, given by

$$\sigma(x) = \begin{cases} 0, & \text{for } x<0,\\ 1, & \text{for } x\geqslant 0.\end{cases} \tag{36}$$

Given$\overline{f}(\tilde{l})$, Eq. (32) can now be rewritten as follows:

$$\begin{aligned}\langle C_{\text{ext}}\rangle &= 2\overline{P}\text{Re}\left\{\int_0^1 [1-\text{e}^{\text{i}kL_{\max}\tilde{L}(m-1)}]\overline{f}(\tilde{L})\,\text{d}\tilde{L}\right\}\\ &= 2\overline{P}\int_0^1 \{1-\text{e}^{-kL_{\max}\tilde{L}m_i}\cos[kL_{\max}\tilde{L}(m_r-1)]\}\overline{f}(\tilde{L})\,\text{d}\tilde{L}.\end{aligned} \tag{37}$$

Eq. (37) is quite similar to Eq. (6) except that the latter is for the extinction cross section of a particle with a specific orientation. From Eq. (37), we can define the cumulative percentage $\overline{q}$ for

the ensemble of the randomly orientated particles as follows:

$$\overline{q}(\tilde{L}) = \int_0^{\tilde{L}} \overline{f}(\tilde{L}')\,\mathrm{d}\tilde{L}'. \tag{38}$$

The cumulative percentage $\overline{q}$ is a monotonic function of $\tilde{L}$. Thus, we can express the scaled projectile-length in the $\overline{q}$ domain as follows:

$$\tilde{L}_{\overline{q}} = \tilde{L}(\overline{q}). \tag{39}$$

Note that $\tilde{L}_{\overline{q}}$ is independent of the physical sizes of the particles in the ensemble as long as the relative size ratio (i.e., the ratio of the size of one particle to another) and morphological shape of the particles remains the same. Based on Eqs. (39) and (40), the extinction and absorption cross sections, after averaging over the ensemble of the particles, are given by:

$$\begin{aligned}\langle C_{\mathrm{ext}}\rangle &= 2\mathrm{Re}\left\{\overline{P}\int_0^1 [1 - \mathrm{e}^{\mathrm{i}kL_{\max}\tilde{L}_{\overline{q}}(m-1)}]\,\mathrm{d}\overline{q}\right\} \\ &= 2\overline{P}\int_0^1 \{1 - \mathrm{e}^{-kL_{\max}\tilde{L}_{\overline{q}}m_i}\cos[kL_{\max}\tilde{L}_{\overline{q}}(m_r - 1)]\}\,\mathrm{d}\overline{q},\end{aligned} \tag{40}$$

and

$$\langle C_{\mathrm{abs}}\rangle = \overline{P}\int_0^1 [1 - \mathrm{e}^{-2kL_{\max}\tilde{L}_{\overline{q}}m_i}]\,\mathrm{d}\overline{q}. \tag{41}$$

The particle orientation information is required only in the computation of $\tilde{L}_{\overline{q}}$. The size independent property of $\tilde{L}_{\overline{q}}$ largely improves the ADT efficiency if various particle sizes are involved.

Fig. 6a shows the scaled projectile-length, $\tilde{L}_{\overline{q}}$, of hexagonal particles with various values of aspect ratio (aspect ratio is defined as $H/2a$ in which H is the length of the particle symmetry axis

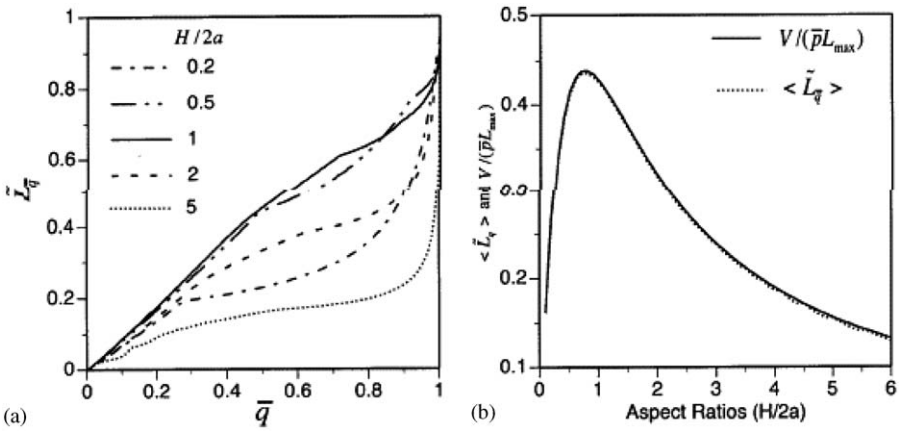

Fig. 6. (a) dimensionless scaled projectile-length $\tilde{L}_{\overline{q}}$ for hexagons with various values of aspect ratios ($H/2a$); (b): the mean value of $\tilde{L}_{\overline{q}}$ and $V/(\overline{P}L_{\max})$.

and a is the semi-width of a particle cross section). It is evident from Fig. 6a that $\tilde{L}_{\overline{q}}$ is quite sensitive to the particle aspect ratio. For a given $\tilde{L}_{\overline{q}}$, the mean scaled projectile-length is given by

$$\langle \tilde{L}_{\overline{q}} \rangle = \int_0^1 \tilde{L}_{\overline{q}} \, \mathrm{d}\overline{q}. \tag{42}$$

Fig. 6b shows the mean scaled projectile-length corresponding to the results shown in Fig. 6a where the ratio $V/(\overline{P}L_{\max})$ is also shown. An interesting point to note is that $\langle \tilde{L}_{\overline{q}} \rangle = V/(\overline{P}L_{\max})$. For example, the mean value of the scaled projectile-length of the hexagonal column with an aspect ratio 2.0, calculated from Eq. (43), is 0.32, which is exactly the value of $V/(\overline{P}L_{\max})$. This feature can be understood via the following relationship:

$$\langle \tilde{L}_{\overline{q}} \rangle = \int_0^1 \tilde{L}_{\overline{q}} \, \mathrm{d}\overline{q} = \int_0^1 \tilde{L} f(\tilde{L}) \, \mathrm{d}\tilde{L} = \frac{\int\int_P L \, \mathrm{d}p}{\overline{P}L_{\max}} = \frac{V}{\overline{P}L_{\max}}. \tag{43}$$

Another interesting feature shown in Fig. 6(b) is that $\langle \tilde{L}_{\overline{q}} \rangle$ as a function of the aspect ratio reaches its maximum when $H = 2a$ (i.e., compact hexagonal particles). Bryant and Latimer [34] developed a simplified version of ADT for randomly orientated particles. They suggested that, in the ADT framework, a randomly orientated particle with a volume V and a projected area $\overline{P}$ can be converted to a cylinder with a thickness of $d_e = V/\overline{P}$ with an incidence normal to the cross section of the cylinder. From the present $\overline{q}$ domain ADT formulation, the projectile-length distribution can be approximated by the following equation:

$$\overline{f}(\tilde{L}) = \delta(\tilde{L} - V/\overline{P}/L_{\max}), \tag{44}$$

where δ is the Dirac delta function. Thus, we have

$$\begin{aligned} \langle C_{\mathrm{ext}} \rangle &= 2\overline{P}\mathrm{Re}\left\{ \int_0^1 [1 - \mathrm{e}^{\mathrm{i}kL_{\max}\tilde{L}(m-1)}]\overline{f}(\tilde{L}) \, \mathrm{d}\tilde{L} \right\} \\ &= 2\overline{P}\mathrm{Re}\left\{ \int_0^1 [1 - \mathrm{e}^{\mathrm{i}kL_{\max}\tilde{L}(m-1)}]\delta(\tilde{L} - V/\overline{P}/L_{\max}) \, \mathrm{d}\tilde{L} \right\} \\ &= 2\overline{P}\{1 - \mathrm{e}^{-kd_e m_i} \cos[kd_e(m_r - 1)]\}, \end{aligned} \tag{45}$$

where d_e is often referred to as the effective size, given by $d_e = V/\overline{P}$. Sun and Fu [15] have shown that the simplified ADT may introduce substantial errors for hexagonal ice crystals.

Fig. 7 shows the extinction and absorption efficiencies of the hexagonal ice crystals with various aspect ratios at a wavelength of $\lambda = 3.7\,\mu\mathrm{m}$ as functions of size parameter $\pi L_{\max}/\lambda$. Here $L_{\max} = (H^2 + 4a^2)^{1/2}$, where H is the length of the symmetry axis of the particle and a is the semi-width of the particle cross section. Because $\overline{f}(\tilde{l})$ is sensitive to the particle aspect ratio, Q_{ext} and Q_{abs} are quite different for the different values of $H/2a$. The left panel of Fig. 7 shows the efficiencies of hexagonal ice crystals with various aspect ratios. For a given size parameter ($\pi L_{\max}/\lambda$), the absorption efficiency of compact hexagonal ice crystals (i.e., $H/2a = 1$) is at the maximum, as is evident from the right panel of Fig. 7. This occurs because $\langle \tilde{L}_{\overline{q}} \rangle$ reaches its maximum values when $H/2a = 1$, as shown in Fig. 6b.

As an example of applying the present ADT formulation to complex particle geometries, Fig. 8 shows the extinction and absorption efficiencies of the bullet rosette ice crystals with various branches at a wavelength of $\lambda = 3.7\,\mu\mathrm{m}$ as a function of size parameter $2\pi r/\lambda$ in which r is the

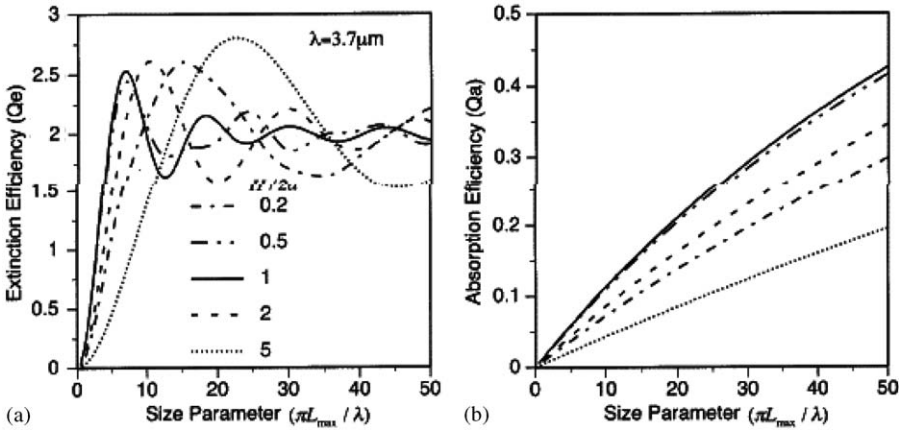

Fig. 7. (a) Extinction efficiencies of hexagons with various aspect ratios; and (b) absorption efficiencies corresponding to Q_{ext} showed in (a).

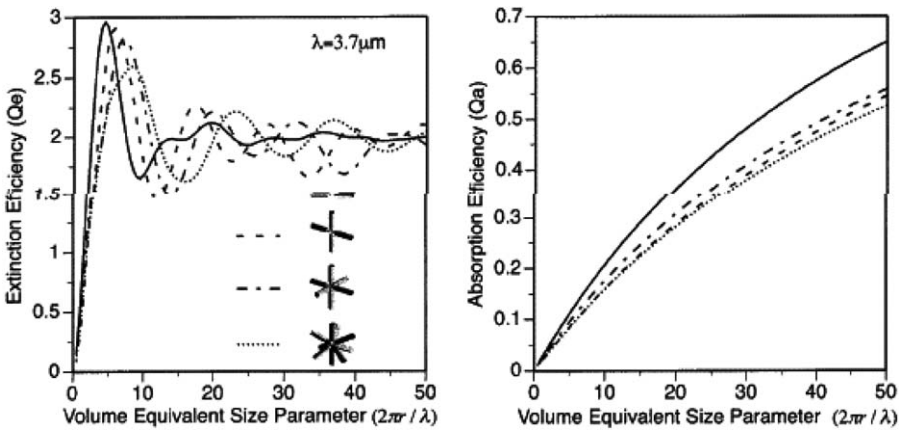

Fig. 8. Extinction and absorption efficiencies of bullet rosettes with various branches.

diameter of the volume-equivalent sphere. The sensitivity of Q_{ext} and Q_{abs} to the number of bullets is evident. In particular, the absorption efficiency decreases with the increase of branch number although the size parameters in Fig. 8 are defined on the basis of volume-equivalence.

3. Modified ADT formulation

The essence of ADT is that the amplitude and polarization of the electromagnetic waves inside an optically tenuous scattering particle is the same as those of the incident wave. Given the geometry shown in Fig. 1, the internal electric field can be expressed as follows:

$$\vec{E}(\vec{r}) = \vec{E}_o \exp(\mathrm{i}k\hat{z} \cdot \vec{r}_o) \exp[\mathrm{i}km\hat{z} \cdot (\vec{r} - \vec{r}_o)]. \tag{46}$$

where $\vec{E}_o$ is the amplitude of the incident electric field, and $\vec{r}_o$ is the position vector of the incident point. From the basic physical principles associated with classic electromagnetic scattering (e.g., Mishchenko et al. [35], Bohren and Huffman [36], Yang and Liou [37] and references cited therein):, the extinction and absorption cross sections can be expressed exactly as follows:

$$C_{\text{ext}} = \text{Im}\left[\frac{k}{E_o E_o^*}(m^2-1)\int\int\int_v \vec{E}(\vec{r}\,')\cdot\vec{E}^*(\vec{r}\,')\,\text{d}^3r'\right], \tag{47}$$

and

$$C_{\text{abs}} = \frac{k}{E_o E_o^*}2m_r m_i\int\int\int_v \vec{E}(\vec{r}\,')\cdot\vec{E}^*(\vec{r}\,')\,\text{d}^3r', \tag{48}$$

where the asterisk denotes the complex conjugate. Using Eq. (47) and integrating the field along projectiles, Eqs. (48) and (49) reduce to

$$C_{\text{ext}} = \text{Re}\left\{(m+1)\int\int_P [1-\text{e}^{\text{i}kl(m-1)}]\,\text{d}p\right\}, \tag{49}$$

and

$$C_{\text{abs}} = m_r\int\int_P (1-\text{e}^{-2klm_i})\,\text{d}p. \tag{50}$$

The preceding expressions for the extinction and absorption cross sections are quite similar to the conventional ADT solutions. In fact, when the refractive index of the particle is close to 1 (i.e., $(m+1)\to 2$ and $m_r\to 1$), the conventional ADT solutions and those given by Eqs. (50) and (51) are essentially the same. However, we note that the extinction efficiently corresponding to Eq. (50) approaches an asymptotic value of $(m+1)$ when the scattering particle is large and strongly absorptive. This is in conflict with the physically correct solution (i.e., an asymptotic solution of 2). The fundamental mechanism for this inaccuracy is that the assumption given by Eq. (47) introduces greater errors for large particles than for small particles. For a small particle, the induced field due to the existence of the particle is weak in comparison with the incident field and Eq. (47) is a good approximation in this case. To overcome this shortcoming in the modified ADT, we rewrite Eqs. (50) and (51) as follows:

$$C_{\text{ext}} = \text{Re}\left\{2\int\int_p [1-\text{e}^{-\text{i}kl(m-1)}]\,\text{d}P + (m-1)\int\int_p [1-\text{e}^{-\text{i}kl(m-1)}]\,\text{d}P\right\}, \tag{51}$$

and

$$C_{\text{abs}} = \int\int_p (1-\text{e}^{-2klm_i})\,\text{d}P + (m_r-1)\int\int_p (1-\text{e}^{-2klm_i})\,\text{d}P. \tag{52}$$

The first terms on the right-hand sides of Eqs. (52) and (53) correspond to the standard ADT solutions, whereas the second terms are associated with errors caused by the approximation for the internal field by Eq. (47) as applied to Eqs. (50) and (51). To ensure that the solutions given by Eqs. (52) and (53) approach their physically correct asymptotic values, we need to add artificial

diffusion terms in Eqs. (52) and (53) in the form of:

$$C_{\text{ext}} = \text{Re}\left\{2\int\int_p [1 - \text{e}^{-\text{i}kl(m-1)}]\,\text{d}P + \text{e}^{-\varepsilon_1 V/\overline{P}}(m-1)\int\int_p [1 - \text{e}^{-\text{i}kl(m-1)}]\,\text{d}P\right\}, \tag{53}$$

and

$$C_{\text{abs}} = \int\int_p (1 - \text{e}^{-2klm_i})\,\text{d}P + \text{e}^{-\varepsilon_2 V/\overline{P}}(m_r - 1)\int\int_p (1 - \text{e}^{-2klm_i})\,\text{d}P, \tag{54}$$

where V and $\overline{P}$ are the particle volume and the oriented averaged projected-area, respectively . The constants ε_1 and ε_2 in Eqs. (54) and (55) are two tuning factors, which can be determined from a comparison of Eqs. (54) and (55) with the corresponding Lorenz-Mie solutions. The values of ε_1 and ε_2 determined in the spherical case can be used as surrogates for nonspherical particles.

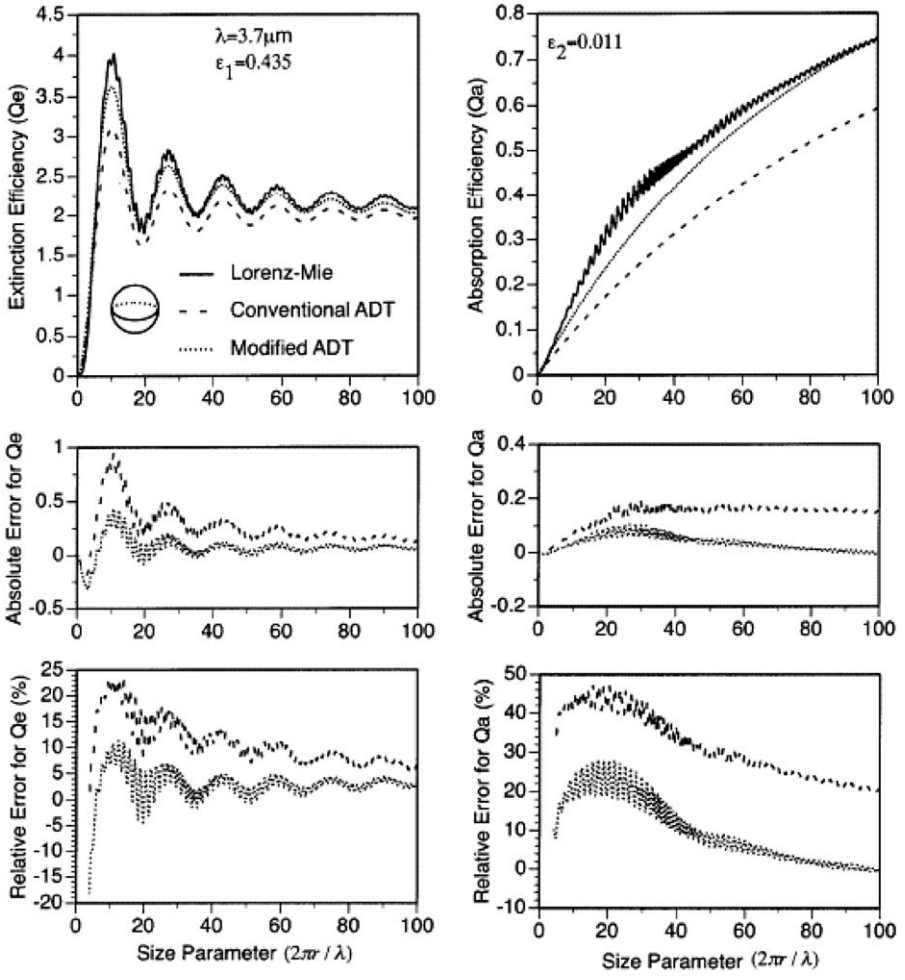

Fig. 9. Extinction and absorption efficiencies of spheres computed for the Lorenz-Mie theory, the conventional ADT, and the modified ADT at a wavelength of 3.7 μm.

Fig. 9 shows the comparison of the values of Q_{ext} and Q_{abs} computed from the Lorenz-Mie theory, the conventional ADT, and the modified ADT. The best fitting values for ε_1 and ε_2 are 0.0435 and 0.011. The absolute and relative error between the ADT method and the exact solutions are defined as follows:

$$Error_{\text{absolute}} = \frac{Q_{\text{exact}} - Q_{\text{ADT}}}{Q_{\text{exact}}}, \tag{55}$$

and

$$Error_{\text{relative}} = \frac{Q_{\text{exact}} - Q_{\text{ADT}}}{Q_{\text{exact}}} \times 100\%, \tag{56}$$

where Q_{exact} represents the Lorenz-Mie solution for the extinction (or absorption) efficiency, and Q_{ADT} represents the corresponding solution from the conventional ADT method or the present modified ADT method. It is evident from Fig. 10 that both absolute and relative errors computed

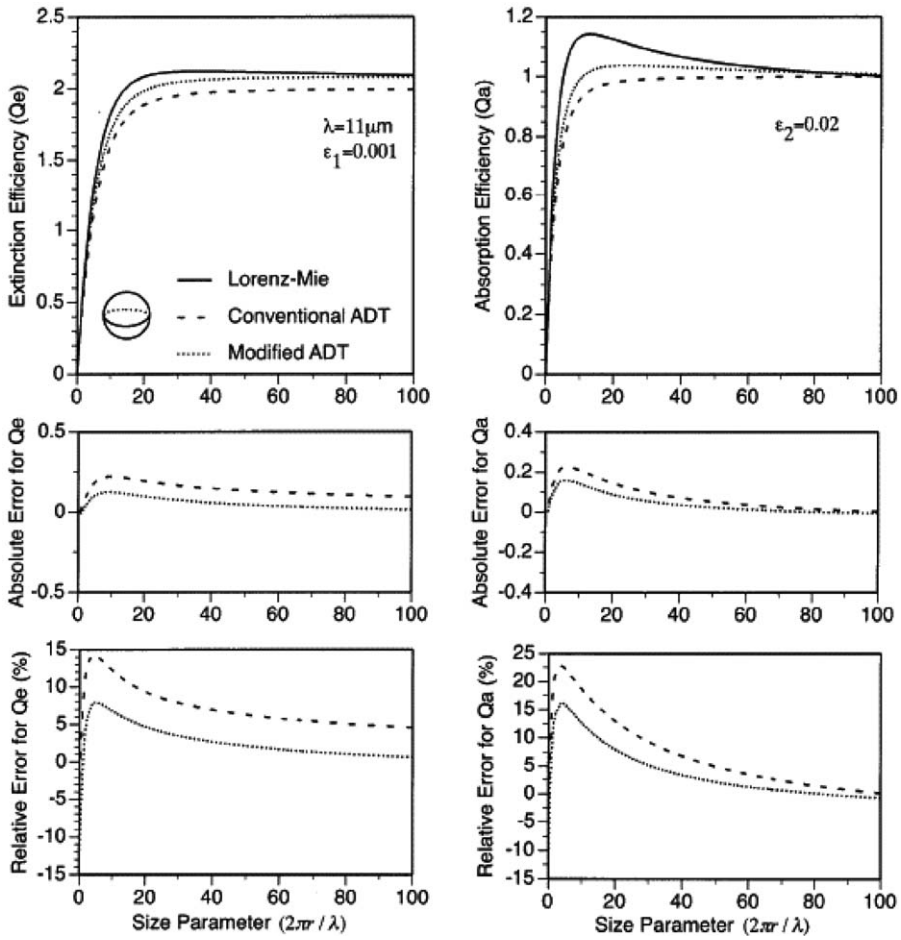

Fig. 10. Same as Fig. 9 except for a wavelength of 11 μm and different tuning factors.

from the present method are much smaller than their conventional counterparts. Note that the absolute error of the modified ADT for Q_{exact} can be slightly larger than that for the conventional ADT when the size parameter is less than 5.

Fig. 10 is similar to Fig. 9 except for a wavelength of 11 μm. The refractive index for the ice at this wavelength is $1.0925 + 0.248i$. Again, it is evident that the modified ADT solution is much more accurate than the conventional ADT results, if the two tuning factors ε_1 and ε_2 are properly selected.

For general nonspherical particles, the tuning factors cannot be known. However, we can use the tuning factors determined for spheres as surrogates for nonspherical particles. To validate this approach, we apply the tuning factors determined for spheres to the case for circular cylinders. Figs. 11 and 12 show the comparisons of the T-matrix solutions [38], the modified ADT solutions,

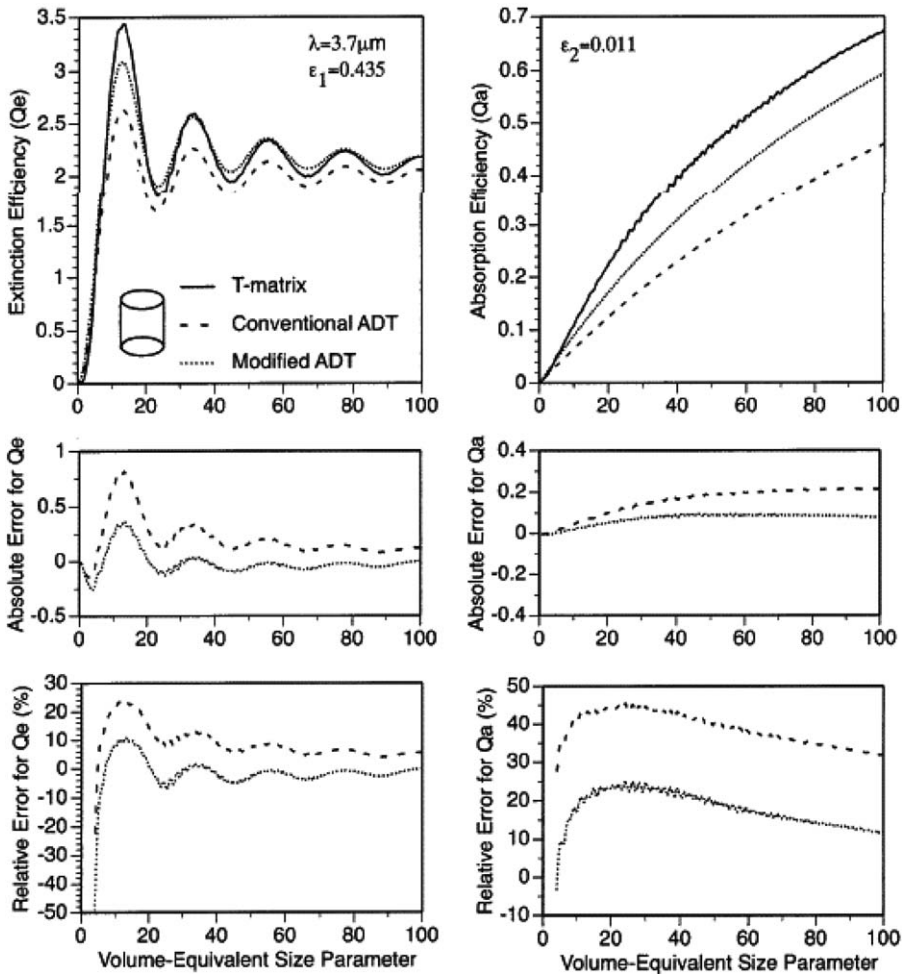

Fig. 11. Extinction and absorption efficiencies computed from the *T*-matrix method [37] and the conventional ADT, and the modified ADT at a wavelength of 3.7 μm. Note that in the modified ADT the tuning factors are same as those shown in Fig. 9 for spheres.

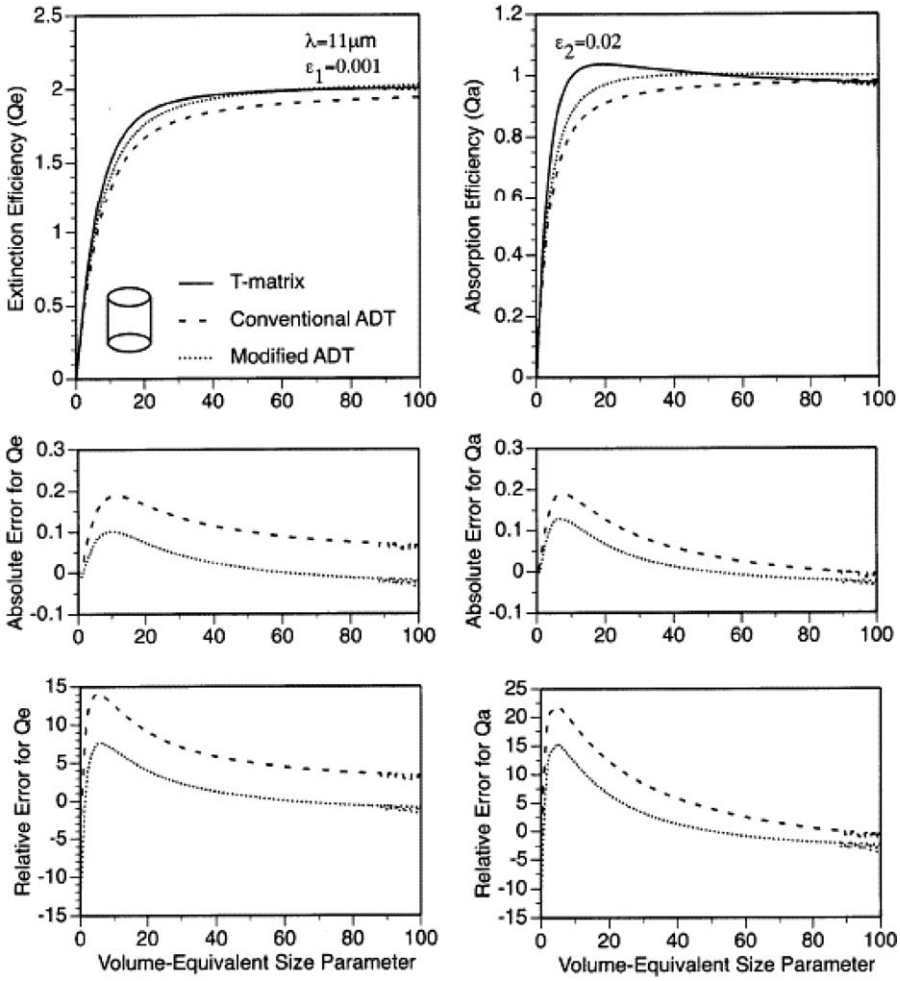

Fig. 12. Same as Fig. 11 except for a wavelength of 11 μm and tuning factors shown in Fig. 10.

and the conventional ADT results. The improvement associated with the modified ADT method is evident from both Figs. 11 and 12.

4. Summary

Recently, Xu et al. [22] and Xu [23] reformulated the conventional ADT by introducing the probability distribution function of the geometric paths of rays inside a scattering particle. In this study, we further enhance their formulae. A scaled projectile length is introduced in the q (the cumulative distribution of the particle projected-area) domain, which is independent of particle physical size as long as the particle shape remains the same (e.g., the projectile-length distribution for a sphere with a 100 μm radius is the same as for a sphere with a radius of 5 μm). The ADT

solutions to the extinction and absorption cross sections can be formulated as integrations with respect to the cumulative projectile-length distribution. In this ADT formulation, the information on particle shape is essentially contained in the dimensionless scaled projectile-length specified in the q domain. We show that the present ADT algorithm is the same as the conventional ADT algorithm for spheres and nonspherical particles under specific and random orientation conditions. We also show the simplified ADT algorithm given by Bryant and Latimer [34] is fundamentally based on a simplification of the projectile-length distribution function in terms of the Dirac delta function.

Furthermore, by assuming that the internal field inside a particle is the same as that in the conventional ADT frame, we develop a modified version of ADT that introduces two tuning factors. These tuning factors can be determined in a spherical case by the best fitting of the ADT solution to the Lorenz-Mie results. For nonspherical particles, the tuning factors obtained in a spherical case can be used as surrogates. This approach is validated in the case for circular cylinders whose optical properties can be obtained by the exact T-matrix method.

Acknowledgements

The authors thank M. I. Mishchenko for using his T-matrix code. This study is supported by a National Science Foundation (NSF) CAREER Award research grant (ATM-0239605) from the NSF Physical meteorology program managed by Dr. William A. Cooper, NASA research grants (NG-1-02002 and NAG5-11374) from the NASA radiation science program managed by Drs. Hal Maring and Donald Anderson, and partially by a subcontract from Science Applications International Corporation (4400053274).

References

[1] Wriedt T. A Review of Elastic Light Scattering Theories. Part Syst Charact 1998;15:67–74.
[2] Mishchenko MI, Hovenier JW, Travis LD, editors. Light Scattering by Nonspherical Particles. San Diego, CA: Academic Press; 2000.
[3] Kahnert FM. Numerical methods in electromagnetic scattering theory. JQSRT 2003;79–80:775–824.
[4] van de Hulst HC. Light scattering by small particles. New York: Wiley; 1957.
[5] Chylek P, Klett JD. Extinction cross sections of nonspherical particles in the anomalous diffraction approximation. J Opt Soc Am A 1991;8:274–81.
[6] Chylek P, Klett JD. Absorption and scattering of electromagnetic radiation by prismatic columns: anomalous diffraction approximation. J Opt Soc Am A 1991;8:1713–20.
[7] Ackerman SA, Stephens GL. The absorption of solar radiation by cloud droplets: an application of anomalous diffraction theory. J Atmos Sci 1987;44:1574–88.
[8] Fournier GR, Evans BTN. Approximation to extinction efficiency for randomly oriented spheroids. Appl Opt 1991;30:2041–8.
[9] Cross DA, Latimer P. General solutions for the extinction and absorption efficiencies of arbitrarily oriented cylinders by anomalous-diffraction methods. J Opt Soc Am 1970;60:904–7.
[10] Stephens GL. Scattering of plane waves by soft obstacles: anomalous diffraction theory for circular cylinder. Appl Opt 1984;23:954–9.

[11] Liu Y, Arnott WP, Hallet J. Anomalous diffraction theory for arbitrarily orientated finite circular cylinders and comparison with exact T-matrix result. Appl Opt 1998;37:5019–30.
[12] Napper DH. A diffraction theory approach to the total scattering by cubes. Kolloid-Z. u. Z.polymere 1966:41–6.
[13] Maslowska A, Flatau PJ, Stephens GL. On the validity of the anomalous diffraction theory to light scattering by cubes. Opt Commun 1994;107:35–40.
[14] Sun WB, Fu Q. Anomalous diffraction theory for arbitrarily oriented hexagonal crystals. JQSRT 1999;63:727–37.
[15] Sun WB, Fu Q. Anomalous diffraction theory for randomly oriented nonspherical particles: a comparison between original and simplified solutions. JQSRT 2001;70:737–47.
[16] Baran AJ, Foot JS, Mitchell DL. Ice crystal absorption: a comparison between theory and implications for remote sensing. Appl Opt 1998;37:2207–15.
[17] Mitchell DL. Parameterization of the Mie extinction and absorption coefficients for water clouds. J Atmos Sci 2000;57:1311–26.
[18] Jones DS. Approximate methods in high-frequency scattering. Proc R Soc London Ser A 1957;239:338–48.
[19] Jones DS. High-frequency scattering of electromagnetic waves. Proc R Soc London Ser A 1957;240:206–13.
[20] Nussenzveig HM, Wiscombe WJ. Efficiency factors in Mie scattering 1980;45:1490–4.
[21] Zhao JQ, Hu YQ. Bridging technique for calculating the extinction efficiency of arbitrary shaped particles. Appl Opt 2003;42:4937–45.
[22] Xu M, Lax M, Alfano RR. Light anomalous diffraction using geometrical path statistics of rays and Gaussian ray approximation. Opt Lett 2003;28:179–81.
[23] Xu M. Light extinction and absorption by arbitrarily oriented finite circular cylinders by use of geometrical path statistics of rays. Appl Opt 2003;42:6710–23.
[24] Goody RM, Yung YL. Atmospheric radiation. Theoretical basis, 2nd ed. New York: Oxford Univ. Press; 1989.
[25] Liou KN. An introduction to atmospheric radiation, 2nd ed. San Diego, CA: Academic Press; 2002.
[26] Chou MD, Kouvaris L. Monochromatic calculations of atmospheric radiative transfer due to molecular line absorption. J Geophys Res 1986;91:4047–55.
[27] Lacis AA, Oinas V. A description of the correlated k distributed method for modeling nongray gaseous absorption, thermal emission, and multiple scattering in vertically inhomogeneous atmospheres. J Geophys Res 1991;96:9027–63.
[28] Fu Q, Liou KN. On the correlated k-distribution method for radiative transfer in nonhomogeneous atmospheres. J Atmos Sci 1992;49:2139–56.
[29] Kratz DP, Cess RD. Infrared radiation models for atmospheric ozone. J Geophys Res 1988;93:7047–54.
[30] Heymsfield AJ, Knollenberg RG. Properties of cirrus generating cells. J Atmos Sci 1972;29:1358–66.
[31] Iaquinta J, Isaka H, Personne P. Scattering phase function of bullet rosette ice crystals. J Atmos Sci 1995;52:1401–13.
[32] Warren S. Optical constant of ice from the ultraviolet to the microwave. Appl Opt 1984;23:1206–24.
[33] Vouk V. Projected area of convex bodies. Nature 1948;162:330–1.
[34] Bryant FD, Latimer P. Optical efficiencies of large particles of arbitrary shape and orientation. J Colloid Interface Sci 1969;30:291–304.
[35] Mishchenko MI, Travis LD, Lacis AA. Scattering, absorption and emission of light by small particles. Cambridge: Cambridge Univ. Press; 2002.
[36] Bohren GF, Huffman DR. Absorption and scattering of light by small particles. New York: Wiley; 1983.
[37] Yang P, Liou KN. Finite-difference time domain method for light scattering by small ice crystals in three-dimensional space. J Opt Soc Am A 1996;13:2072–85.
[38] Mishchenko MI, Travis LD. Capabilities and limitations of a current FORTRAN implementation of the T-matrix method for randomly oriented, rotationally symmetric scatterers. JQSRT 1998;60:309–24.